

TECNIACÚSTICA 2017

48º CONGRESO ESPAÑOL DE ACÚSTICA
48º CONGRESSO ESPANHOL DE ACÚSTICA
48th SPANISH CONGRESS ON ACOUSTICS

ENCUENTRO IBÉRICO DE ACÚSTICA
ENCONTRO IBÉRICO DE ACÚSTICA
IBERIAN ENCOUNTER ON ACOUSTICS

4 - 6, octubre / Outubro / October, 2017

EUROPEAN SYMPOSIUM ON UNDERWATER ACOUSTICS APPLICATIONS

3, octubre / Outubro / October, 2017

EUROPEAN SYMPOSIUM ON SUSTAINABLE BUILDING ACOUSTICS

5, octubre / Outubro / October, 2017

Sede / Venue Congress and Symposium on Sustainable Building Acoustics
Escuela Universitaria de Arquitectura Técnica de A Coruña
Universidad de A Coruña
Campus da Zapateira s/n.
15071 A Coruña

Sede / Venue Symposium on Underwater Acoustics Applications
Centro Universitario de la Defensa. Escuela Naval Militar de Marín
Plaza de España, s/n,
36920 Marín, Pontevedra

Editores / Editors
Antonio Calvo-Manzano (SEA)
Antonio Pérez-López (SEA)

© Copyright: Sociedad Española de Acústica -SEA-

ISBN: 978-84-87985-29-4
ISSN: 2340-7441 (Versión Digital)

TECNIACUSTICA A CORUÑA · 2017

48º CONGRESO ESPAÑOL DE ACÚSTICA
ENCUENTRO IBÉRICO DE ACÚSTICA
EUROPEAN SYMPOSIUM ON UNDERWATER ACOUSTICS APPLICATIONS
EUROPEAN SYMPOSIUM ON SUSTAINABLE BUILDING ACOUSTICS

FUERZA DE RADIACIÓN EN HACES FOCALIZADOS DE ULTRASONIDOS DE AMPLITUD MODULADA

PACS: 43.25-x

Jiménez Noé[1]; Camarena Francisco[1]; González-Salido Nuria[2]; Jiménez-Gambín Sergio[1].
[1]: Instituto de Instrumentación para Imagen Molecular (I3M),
Centro Mixto Universitat Politècnica de València. Consejo Superior de Investigaciones Científicas.
Camino de Vera s/n,
46022 Valencia. España
Tel: 962 849 300 (43148)
E-Mail: fcamarena@fis.upv.es
[2]: ITEFI, Spanish National Research Council (CSIC)
Serrano 144
28006 Madrid. España

Palabras Clave: Nonlinear acoustics; Acoustic radiation force; Finite-amplitude acoustic beams

ABSTRACT

The phenomenon of the displacement of the position of the pressure, intensity and acoustic radiation force maxima along the axis of focused acoustic beams under increasing driving amplitudes (nonlinear focal shift) is studied for the case of a moderately focused beam excited with continuous and 25 kHz amplitude modulated signals, both in water and tissue. We prove that in amplitude modulated beams the linear and nonlinear propagation effects coexist in a semi-period of modulation, giving place to a complex dynamic behavior, where the singular points of the beam (peak pressure, rarefaction, intensity and acoustic radiation force) locate at different points on axis as a function of time. These entire phenomena are explained in terms of harmonic generation and absorption during the propagation in a lossy nonlinear medium both for a continuous and an amplitude modulated beam. One of the possible applications of the acoustic radiation force displacement is the generation of shear waves at different locations by using a focused mono-element transducer excited by an amplitude modulated signal.

RESUMEN

Se estudia el fenómeno del desplazamiento de la posición de los máximos de presión, intensidad y fuerza de radiación acústica a lo largo del eje de un haz de ultrasonidos de focalización intermedia cuando se aumenta la amplitud de excitación. El estudio se plantea en propagación en agua y en tejido, y con haces de amplitud modulada, que presentan efectos lineales y no lineales en un semiperiodo de modulación. Demostramos que esta circunstancia da lugar a una dinámica compleja, donde los puntos singulares del haz: presión y rarefacción máximas, intensidad y fuerza de radiación acústica se distribuyen en diferentes puntos a lo largo del eje axial en función del tiempo. Se explica el fenómeno en base a la generación de harmónicos y a la absorción durante la propagación en un medio no lineal. Una de las posibles aplicaciones del desplazamiento de la fuerza de radiación acústica es la generación de ondas transversales mediante el uso de un transductor mono-elemento excitado con una señal de amplitud modulada.

1. Introduction

The study of the acoustic field generated by focusing sources in the nonlinear regime is a continuously developing area of research as finite amplitude sound beams are increasingly used in medicine and industry [1–5]. Nonlinear propagation implies asymmetric wave steepening, progressive harmonic generation, nonlinear absorption, sound saturation, self-refraction and selfdemodulation [6]. All these nonlinear effects change the spatial distribution of the acoustic field with respect to the linear case, i.e., among other things, the location of the on-axis peak compression and rarefaction pressure, intensity and acoustic radiation force (ARF), as well as the focal spot dimensions.
The nonlinear focal shift phenomenon, defined as the shift of the maximum pressure (and also intensity and ARF) position along the axis of focused acoustic beams under increasing driving voltages, has been discussed and interpreted in previous works [7-11]. The location of the singular points of a focused ultrasonic beam, i.e., the on-axis maximum and negative pressure, maximum intensity and ARF, depends on the nonlinear degree of the propagated waves. This is especially relevant in moderately-focused beams since the focusing is high enough to make the nonlinear effects relevant, but at the same time the transversal area of the focus is not as small as in highly focused devices, making the self-refraction effect to play an important role [6,11]. The singular points of a beam (as for example the location of the maximum ARF) generated by a moderately focused mono-element emitter can be moved just by raising the amplitude of the voltage applied to the source. One of the applications that comes to mind is to generate a supersonic source of shear waves [12] with a focused mono-element transducer for elasticity imaging applications.
The aim of this work is to investigate experimentally and numerically the dynamic behavior of the singular points of a moderately focused beam operating from linear to nonlinear regime, and excited with amplitude modulated (AM) and continuous signals. Both in water and soft tissue (human liver) media were considered.

2. Materials and methods

2.1. Experimental set-up

The experimental set-up for the pressure measurements in water follows the classical scheme of confronted emitting focused source and receiving calibrated membrane hydrophone, located inside a(0.75; 0.6; 0.5) m water tank filled with degassed and distilled water at 26 C, as shown in Fig. 1. The ultrasound source was formed by a plane single element piezoceramic crystal (PZ 26, Ferroperm Piezoceramics, Denmark) mounted in a custom designed stainless-steel housing and a poly-methyl methacrylate (PMMA) focusing lens with aperture 2a= 50 mm and radius of curvature R= 70 mm. The resonant frequency of the transducer was fo=1.112 MHz, and it was driven by a signal generator (14 bits, 100 MS/s, model PXI5412, National Instruments) and amplified by a linear RF amplifier (ENI 1040L, 400 W, +55 dB, ENI, Rochester, NY). The pressure field was measured by a PVDF membrane hydrophone with a 200 lm active diameter (149.6 mV/MPa sensitivity at 1.112 MHz, Model MHB-200, NTR/Onda) calibrated from 1 MHz to 20 MHz). The hydrophone signals were digitized at a sampling rate of 64 MHz by a digitizer (model PXI5620, National Instruments) averaged 500 times to increase the signal to noise ratio. An x-y-z micro-positioning system (OWIS GmbH) was used to move the hydrophone in three orthogonal directions with an accuracy of 10 lm. All the signal generation and acquisition process was based on a NI8176 National Instruments PXI-Technology controller, which also controlled the micro-positioning system. Temperature measurements were performed throughout the whole process to ensure no temperature changes of 0.6 ºC.

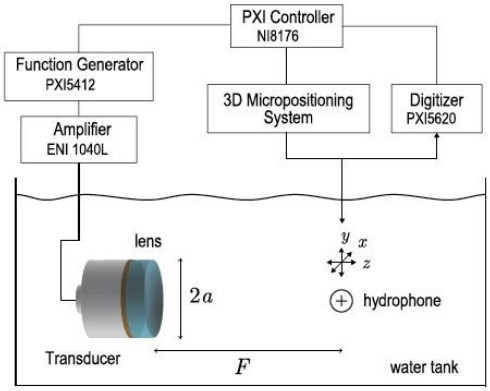


Fig. 1. Scheme of the experimental set-up for the pressure measurement in water.

2.2. Linear characterization of the beam

To accurately determinate the position of the radiator axis, a variant of the procedure described in Cathignol et al. [16] was developed. Firstly, the transducer was oriented along the z-axis of the micro-positioning system. In order to find the focal region of the transducer, the maximum pressure distribution generated by a 20-cycles sinusoidal pulsed burst was measured along the axis of the radiator. These measurements provided a rough estimation of the transducer focal area. Then, the pressure waveforms p.t; x; y; z. were measured at the focal area in five planes along the z axis of the micro-positioning system, separated Dz= 5 mm. Waveforms were acquired along these planes in planes of 6mmx6mm (x-y directions) at 0.5 mm spatial resolution (144 measurement points per plane)..

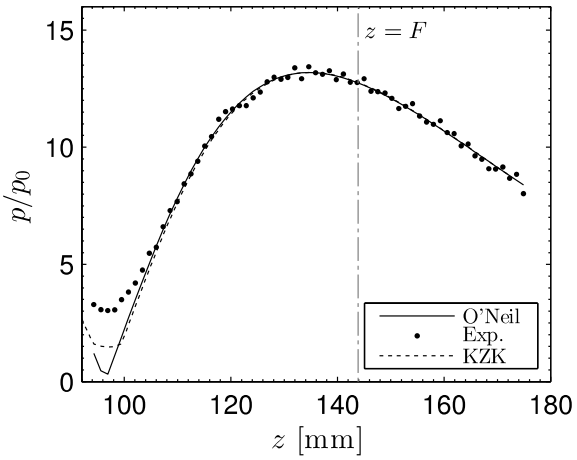


Fig. 2. On-axis maximum pressure distribution for small amplitude wave propagation obtained by experimental data (dots), O'Neill solution (solid line) and KZK numerical solution (dotted line). The vertical dashed-dotted line shows the position of the geometric focus.

The geometrical focal length (considering the PMMA focusing lens) and the aperture of the transducer were nominally rated by the manufacturer as F= 157 mm and 2a= 50 mm, respectively. The results of both the O'Neil model and the one calculated with the "best fit" aperture and geometrical focal length in the KZK simulation are in good agreement with the experimental data, as shown in Fig. 2.

2.3. Measurement procedure

To study the nonlinear focal shift produced by continuous and AM beams, the acoustic field on the radiator axis was measured for different initial pressures. Firstly, the transducer was excited

by a 40 cycles-sine wave burst with 27 values of amplitude with voltages ranging from 5 Vp to 228 Vp (assuming a source pressure amplitude linearly proportional to the driving voltage from po= 2.63 kPa to po= 120 kPa). Then, the experiment was repeated for an AM beam generated by the 25 kHz modulation of a continuous beam (90 cycles-sine wave burst). The on-axis intensity distribution and ARF was evaluated according to the procedure explained in [13].

2.4. Numerical model

Numerical modeling of the experimental conditions was performed by using the numerical solution of the KZK nonlinear parabolic equation over a cylindrical axisymmetric coordinate system. This model takes into account the nonlinearity, diffraction (assuming a beam in the paraxial/parabolic approximation), thermo-viscous absorption and relaxation [6].

3. Results

3.1. Dynamic nonlinear focal shift in water

The amplitude variation along the temporal profile of the 25 kHz-AM signal (see Fig. 3(a)) involves the coexistence of the linear regime propagation for periods with small amplitude (without distortion; see Fig. 3(b)) and the nonlinear regime propagation for the central periods (with large amplitude and distortion; see Fig. 3 (c)) during the propagation of the wave. This results in dynamic focal shifts during the application of the signal, as can be seen in Fig. 4 for the peak pressure, intensity and ARF. These results show that the focusing characteristics of the beam can change in time when we modulate the excitation signal. Fig. 4 represents the highest excitation value reached in the experiment: 228 Vp in the transducer and a peak pressure of 2.02 MPa at the focus. The dynamic process proceeds as follows: first, the low amplitude cycles of the AM beam focus on a point around 136 mm from the source according to the medium properties and the source's physical characteristics: frequency, aperture, and geometrical focal length [9]. Then, as the local amplitude of the AM signal reaches nonlinear regime in the central part of the AM packet (see Fig. 3(c)), the focal maxima moves away from the source. As shown, a different focal-shift behavior was obtained for pressure, ARF and intensity.

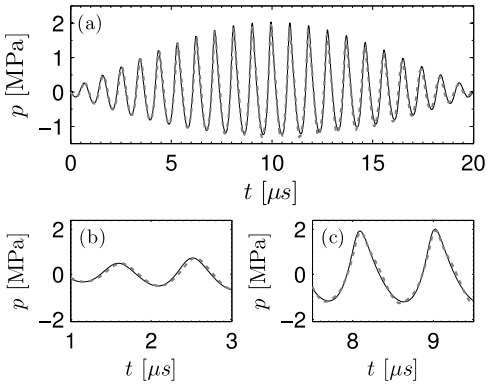


Fig. 3. Experimental (dashed line) and KZK simulated (continuous line) waveform measured at The input voltage in the experiment was 228 Vpp and the initial pressure in simulation was 105 kPa, chosen to produce equal pressure at the focus. (a) Complete half-period of the AM signal, where linear and nonlinear propagation coexist at different times. (b) Initial small-amplitude oscillations and (c) central oscillations of the AM signal, where strong nonlinearities are produced.

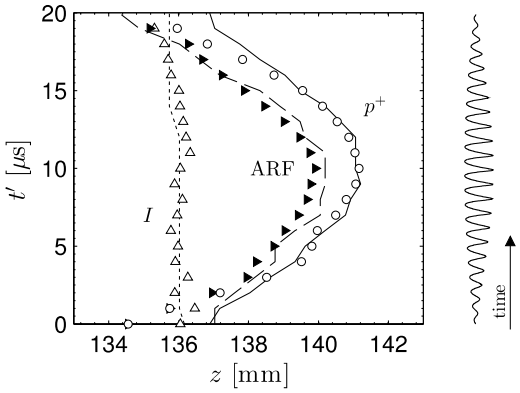


Fig. 4. On-axis simulated (lines) and experimental (markers) of the peak pressure (white circles), maximum intensity (white triangles) and maximum ARF (Black triangles) locations obtained for each period of the AM-carrier component. t0 is the dimensionless retarded time, where the time delay due to wave propagation distance has been eliminated.

As no shock waves were present in our experiment, we explored the strong nonlinear regime of

propagation in an AM modulated beam by means of a KZK simulation. Fig. 5 shows the nonlinear shift in two scenarios (moderate nonlinear regime: 2.02 MPa at the focus, which corresponds with the maximum excitation in our experiment) and 9.4 MPa at the focus (strong nonlinear regime). The strong nonlinear scenario presents more complex dynamics than the moderate one. The maximum displacement of the focus was 12.5 mm for positive pressure, 8.1 mm for rarefaction pressure, 3.4 mm for intensity and 15.1 mm for ARF. The maximum position of the pressure exceeds the geometrical focus by 4.2 mm, and the ARF one by 6.7 mm. However, when the signal amplitude is high enough to produce shock waves in the propagation, the focus returns to the transducer in both cases. This happens when the central part of the AM packet is propagating through the media, and is due to the effect of the nonlinear absorption associated with shock waves, which saturates the harmonic generation processes.

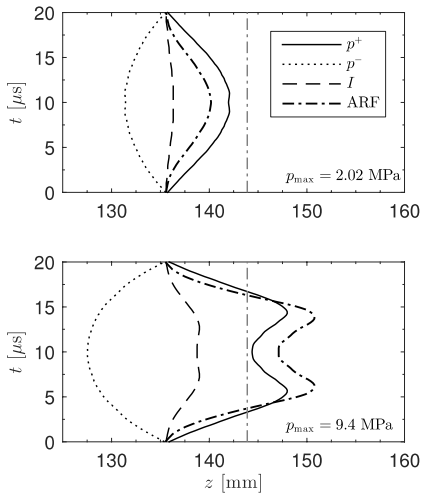


Fig. 5. On-axis dynamic focal displacements in water for a 25 kHz AM signal. Top: moderate nonlinear regime. Bottom: strong nonlinear regime. Peak pressure (solid line), rarefaction minimum (dashed line), intensity (dotted line) and ARF (dasheddotted line). The vertical dashed line shows the geometric focus. (a) Weakly nonlinearity scenario, (b) strongly nonlinear scenario.

3.3. Dynamic nonlinear focal shift in liver

Multiple relaxation and inhomogeneities were introduced in the KZK model to simulate the propagation of the beam through a layer of soft-tissue (human liver). A set of seventy simulations were performed for amplitudes that ranged from the linear to strongly nonlinear regime. Fig. 6 shows the location of the Peak pressure, each harmonic, intensity and ARF. First, it can be observed that in the linear regime the focus is shifted towards the source due to the strong attenuation, where all the magnitudes peak at z= 127.7 mm (compared to 135.6 mm obtained in water). The linear position of the focus is located at 127.7 mm from the transducer, 8.3 mm before the focus obtained in water (136 mm). This effect is produced by the medium absorption in conjunction with an elongated focal area. Due to the high f-number of the source (2.57), the focal area, defined as the acoustic field area that exceeds 1/2 of the Peak intensity, has an axial length of 45λ. During propagation through the focal area, where locally plane waves can be considered, the wave suffers from exponential decay. On this path a total attenuation of 3.2 dB is observed in tissue (considering 0.5 dB/cm/MHz the absorption of the liver [26]), so the peak pressure is located at the initial part of the focal area (127.7 mm) instead of at its location in weakly absorbing media such as water (136 mm). Despite this effect, in the weakly nonlinear regime (p+ < 2 MPa) the nonlinear behavior of the peak pressure and intensity in soft-tissue is almost the same as in thermo viscous media, in which each harmonic is progressively generated throughout the propagation and each one focus farther away than the previous one. However, the ARF shows a different behavior. ARF is also calculated by adding

the intensities of the harmonics corrected each one by a factor proporcional to its absorption. In soft-tissues the absorption follows a frequency power-law with an exponent γ=1, (in contrast with thermo viscous fluids where γ=2). Therefore, as regards the ARF, higher harmonics have less relative importance to the fundamental one in tissue than in an equivalent thermoviscous media with γ=2. Due to this, the observed focal shift of the ARF in human-liver is more relaxed than in water, as shown in Fig. 6. In the present case the ARF peak location falls between the maximum intensity and peak pressure location.

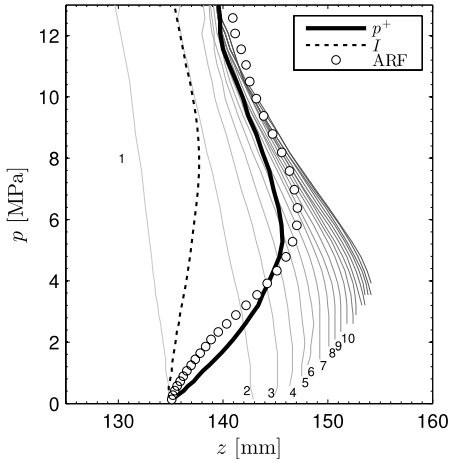


Fig. 6. (a) On-axis maximum pressure, p., intensity, I., and ARF location obtained from the KZK simulation of the ultrasonic beam in tissue. Numbered gray lines represent the on-axis maximum pressure location of each harmonic. (b) Axial pressure profiles for increasing source amplitude, p0 (increasing from gray to black). The thick black line shows the peak pressure location, p.. The vertical dashed dotted line marks the geometrical focal.

Then, in the moderately nonlinear regime ($2 < p^+ < 4$ MPa), it can be observed that the beam's self-defocusing effect grows with amplitude. The velocity of a finite amplitude perturbation depends on the wave amplitude, and for a focused beam the amplitude is higher along the propagation axis than in remote regions. Therefore, the compressive phases of the wave travel faster near the axis. Consequently, a flattening of the wave front is produced and a defocusing effect is observed: the pressure maximum is shifted from the source. The contrary effect is produced for the rarefaction phase of the waveform. Up to $p^+ < 6$ MPa, a total shift of 2.5 mm was observed for the intensity, while it was 9.4mm for the peak pressure and 7.6 mm for the ARF. Note that these values are almost double those in water.

For higher amplitudes, the waveforms at the focal become strongly asymmetric: the compression region becomes sharper with high amplitude and the rarefaction region smoother with lower amplitude. On the one hand, when these asymmetric shocks are present, the Rankine-Hugoniot jump conditions lead to an acceleration of the shock front near the axis in the focal area. As the shock-front Speedy increases, it becomes flattened. Again, the beam is self-refracted and this nonlinear self-action phenomena produces the de-focusing of the beam: the pressure maxima shifts. On the other hand, when shocks are present, nonlinear absorption is produced: the wave amplitude decreases sharply with distance. Therefore, it produces the opposite effect and the observed displacement of the peak pressure returns towards the source, as shown in Fig. 6

As before, 25 kHz-AM excitation signals were applied in two scenarios: moderate and strongly nonlinear propagation. The inicial pressure values were chosen to produce similar pressure

amplitudes at the focus as in the case of water: po= 0.26 MPa amplitude excitation at the source surface, which leads to a Peak pressure of p+= 2.9 MPa (moderate nonlinear scenario); and po= 0.69 MPa on the transducer surface, which leads to a Peak pressure of p+= 9.5 MPa (strongly nonlinear scenario).

Fig. 7 shows the dynamic location of the on-axis positive pressure, minimum rarefaction and intensity maxima. In the moderate scenario, as shown in Fig. 7(a), the shifts are shorter than those obtained in water: 5.4 mm for peak pressure, 3.5 mm for Peak negative pressure, 0.7 mm for intensity and 2.3 mm for the ARF, i.e., 15% lower for pressure, 30% for the intensity, and 50% for the ARF observed in water. The high value of the absorption in liver (0.5 dB/cm) compared to the absorption in water (0.002 dB/cm) drastically reduces the amplitude of the harmonics, and consequently the nonlinear shift effect.

Fig. 7(b) shows the dynamic nonlinear focal shift results for the strongly nonlinear scenario in human liver. A displacement of .9.3 mm for peak pressure is obtained, 7.1 mm for rarefaction pressure, 2.5 mm for intensity and 7.6 mm for the ARF. The maximum on-axis pressure location does not exceed the geometrical focus because the linear focus is closer to the emitter (127.7 mm) than in water, as explained above. In this case, the recoil in the shift is also observed in the central part of the AM packet, but is smaller than in water: the strong absorption in tissue makes it more difficult to generate shock waves in the pre-focal region.

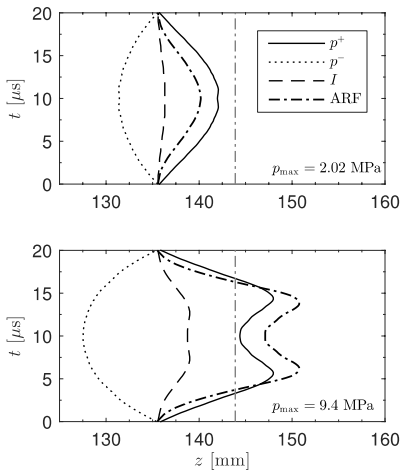


Fig. 7. On-axis focal displacements for a 25 kHz-AM beam in liver. Peak pressure (solid line), rarefaction minimum (dashed line), intensity (dotted line). The vertical dashed line shows the geometrical focus. (a) Weakly nonlinear scenario, (b) strongly nonlinear scenario.

4. Conclusions

This paper describes the analysis of the nonlinear behavior of the on-axis maximum pressure, intensity and ARF in a 25 kHz AM beam (emitter characteristics: f-number = 2.6 and fo=1.112 MHz). The pressure fields were measured in water and compared to those obtained from the numerical results based on the KZK equation, obtaining a good agreement between experimental and numerical data. The results obtained demonstrate the ability of nonlinear AM beams generated with a mono element transducer to produce dynamical axial focal displacements. The linear and nonlinear propagation regimes, together with shock waves and nonlinear absorption coexist during the semi-period of modulation of the beam (20 μs in our case). The same results, but with reduced magnitude, have been observed in a KZK simulation of the beam propagating in human liver. Acoustic radiation force, and especially dynamic ARF, is widely used in many elasticity Imaging techniques to induce displacements of tissue [14], or to remotely induce shear waves inside the medium [15]. We have observed that for amplitude-modulated beams, the

position of maximum ARF changes with time, following the modulation function. Although the focusing degree of the devices used in these imaging techniques is considerably higher than the one considered in the present study, and as a consequence the nonlinear shift effects are lower in these image techniques, they can be important enough to affect the calculation of the elastic characteristic of the tissue. Future research will continue in this line. Finally, the phenomenology found in this work leads us to consider the possibility of exploring the generation of supersonic shear waves by means of a mono-element transducer excited by the appropriate amplitude-modulated signal: the frequency modulation would define the speed of the ARF displacement, while the maximum amplitude would fix the total distance covered.

Acknowledgements
FC acknowledge financial support from the AICO/2016-108 program of the Generalitat Valenciana. NJ acknowledge financial support from the FPI Grant PAID-2011 from the Universitat Politècnica de València. NGS acknowledge financial support from DPI2013- 42236 R Project of the Spanish Ministry of Economy and Competitiveness, S2013/MIT-3024 of the Community of Madrid and from FPU Grant 12/02187 from the Spanish Ministry of Education, Culture and Sport.

References
[1] N. Bakhvalov, Y.M. Zhileikin, E. Zabolotskaya, R. Khokhlov, Focused highamplitude sound beams, Sov. Phys. Acoust. 24 (1978) 10–15.
[2] B.G. Lucas, T.G. Muir, The field of a focusing source, J. Acoust. Soc. Am. 72 (1982) 1289–1296.
[3] F.A. Duck, H.C. Starritt, The locations of peak pressures and peak intensities in finite amplitude beams from a pulsed focused transducer, Ultrasound Med. Biol. 12 (1986) 403–409.
[4] J. Blitz, G. Simpson, Ultrasonic Methods of Non-destructive Testing, vol. 2, Springer Science & Business Media, London, 1995.
[5] F.A. Duck, A.C. Baker, H.C. Starritt, Ultrasound in Medicine, CRC Press, 1998.
[6] M. Hamilton, D. Blackstock, Nonlinear Acoustics, Academic Press, San Diego, CA 92101, USA, 1998.
[7] N. Bakhvalov, Y.M. Zhileikin, E. Zabolotskaya, Nonlinear propagation of sound beams with a uniform amplitude distribution, Sov. Phys. Acoust. 26 (1980) 95– 100.
[8] M.A. Averkiou, M.F. Hamilton, Nonlinear distortion of short pulses radiated by plane and focused circular pistons, J. Acoust. Soc. Am. 102 (1997) 2539–2548.
[9] Y.N. Makov, V. Sánchez-Morcillo, F. Camarena, V. Espinosa, Nonlinear change of on-axis pressure and intensity maxima positions and its relation with the linear focal shift effect, Ultrasonics 48 (2008) 678–686.
[10] O. Bessonova, V. Khokhlova, M. Bailey, M. Canney. Focusing of high power ultrasound beams and limiting values of shock wave parameters, Acoust. Phys. 55 (2009) 463–473.
[11] F. Camarena, S. Adrián-Martínez, N. Jiménez, V. Sánchez-Morcillo, Nonlinear focal shift beyond the geometrical focus in moderately focused acoustic beams, J. Acoust. Soc. Am. 134 (2013) 1463–1472.
[12] J. Bercoff, M. Tanter, M. Fink, Supersonic shear imaging: a new technique for soft tissue elasticity mapping, IEEE Trans. Ultrason. Ferroelectr. Freq. Control 51 (2004) 396–409.
[13] Noé Jiménez, Francisco Camarena,Nuria González-Salido. Dynamic nonlinear focal shift in amplitude modulated moderately focused acoustic beams. Ultrasonics 75 (2017) 106–114.
[14] C. Maleke, M. Pernot, E.E. Konofagou, Single-element focused ultrasound transducer method.
[15] K.R. Nightingale, M.L. Palmeri, R.W. Nightingale, G.E. Trahey, On the feasibility of remote palpation using acoustic radiation force, J. Acoust. Soc. Am. 110 (2001) 625–634.